doi.org/10.36721/PJPS.2025.38.4.REG.13103.1

Unearthing novel PPAR-γ activators: *In silico* design of eucalyptol analogues for ulcerative colitis

Ozair Khurram Hashmi[1], Muhammad Hanzla[1], Calvin R. Wei[2], Muhammad Aashir Khan[1], Muhammad Wassam Bin Wasim[1], Muhammad Abdullah[1], Syed Hafiz Ahmed[1] and Muhammad Osama*[1,3]

[1]Department of Pharmacy Practice, Faculty of Pharmacy and Pharmaceutical Sciences, University of Karachi, Karachi, Pakistan
[2]Department of Research and Development, Shing Huei Group, Taipei, Taiwan
[3]Department of Pharmacology, Faculty of Pharmacy and Pharmaceutical Sciences, University of Karachi, Karachi, Pakistan

Abstract: Ulcerative colitis (UC) is a chronic inflammatory bowel disease with rising prevalence, necessitating novel therapeutics. The peroxisome proliferator-activated receptor gamma (PPAR-γ) is a promising target for UC management. This study aimed to identify potent, selective PPAR-γ agonists derived from the natural product eucalyptol (1,8-cineole), with reported anti-inflammatory and PPAR-γ activating properties but limited clinical utility. A computational workflow encompassing molecular docking of 342 eucalyptol analogues against PPAR-γ, pharmacokinetic prediction, and molecular dynamics simulations was employed. Docking revealed five top-scoring hits with higher predicted PPAR-γ binding affinities than eucalyptol. AA051 emerged as the most promising candidate, exhibiting the lowest binding free energies (-31.16 kcal/mol MMGBSA, -16.53 kcal/mol MMPBSA), favorable ADMET profiles including oral bioavailability, solubility, blood-brain barrier permeability, and conformational stability. AA055 also showed a promising binding profile albeit with initial instability. This study highlights computational approaches in drug discovery, identifying AA051 as a compelling PPAR-γ agonist lead for UC therapy, paving the way for experimental validation and optimization of this novel scaffold.

Keywords: PPAR, agonist, ulcerative colitis, molecular docking, molecular dynamic, ADMET, natural Products

Submitted on 11-07-2024 – Revised on 12-03-2025– Accepted on 12-07-2025

INTRODUCTION

Ulcerative colitis (UC) is a prominent subtype of inflammatory bowel disease (IBD), characterized by chronic colonic inflammation. Clinical manifestations of UC encompass diarrhea, hematochezia (bloody stools), weight loss, abdominal cramping, pyrexia (fever), and lassitude (fatigue) (Gajendran *et al*., 2019). The etiology of IBD is multifactorial, encompassing genetic predisposition, immune system dysregulation, gut microbiome imbalance, and environmental influences (Decara *et al*., 2020). Current therapeutic options for UC include aminosalicylates, corticosteroids, immunosuppressants, and biologics. While these therapies can induce remission, they are often associated with severe side effects, high costs, or reduced efficacy in maintaining long-term remission (Ferretti *et al*., 2022). These limitations underscore the urgent need for novel, safe, and effective therapeutic agents.

The nuclear receptor peroxisome proliferator-activated receptor gamma (PPARγ) has emerged as a key therapeutic target in UC (Bertin *et al*., 2013; Fang *et al*., 2021). PPARγ is highly expressed in colonic epithelial cells and regulates critical processes such as lipid metabolism, glucose homeostasis and the attenuation of inflammatory responses. Activation of this receptor has been shown to restore epithelial integrity, suppress pro-inflammatory cytokine release, and improve colonic barrier function (Caioni *et al*., 2021; Kim *et al*., 2023, Wei *et al*., 2025). These properties make PPARγ an attractive candidate for drug development in UC.

Eucalyptol (1,8-cineole), a natural monoterpene found in essential oils such as eucalyptus, rosemary, and tea tree, has been identified as a potential PPARγ agonist with anti-inflammatory properties (Hoch *et al*., 2023). A recent study by Venkataraman *et al*. has demonstrated its ability to modulate PPARγ and alleviate colon inflammation in preclinical models (Venkataraman *et al*., 2023). However, despite its therapeutic potential, eucalyptol has inherent limitations, including suboptimal binding affinity, limited pharmacokinetic properties, and potential toxicities. These drawbacks hinder its clinical application as a standalone therapeutic agent (Izham *et al*., 2021).

To address these challenges, this study focuses on designing and testing new eucalyptol analogues that target PPARγ. Structural changes were made to improve binding strength, pharmacokinetic properties, and reduce toxicity. An in-silico process, including molecular docking, and ADMET analysis, was used to find lead compounds with better performance than the parent eucalyptol molecule. The main goals of this study are to analyze how well

**Corresponding author:* e-mail: osama_hum@hotmail.com

eucalyptol analogues bind to PPARγ and interact with it using molecular docking, assess the pharmacokinetic and toxicity profiles of these analogues using computational ADMET tools, and identify lead compounds that combine strong effectiveness with safety for further preclinical development. This approach provides a framework for future drug discovery efforts.

MATERIALS AND METHODS

Analysis of crystalline structure

Following a comprehensive literature review, a specific receptor was chosen for docking simulations. The crystal structure of Peroxisome Proliferator-Activated Receptor gamma (PPARγ) was retrieved from the Protein Data Bank (PDB) using accession code 4A4W [RCSB Protein Data Bank, (rcsb.org) (Venkataraman *et al*., 2023). The protein structure was then subjected to a comprehensive validation process utilizing web-based servers. This included evaluations for chirality, Ramachandran analysis of φ (phi) and ψ (psi) dihedral angles, planarity, disulfide bond formation, covalent geometry, non-bonded interactions, stereochemical parameters, and main-chain hydrogen bonding patterns. PROCHECK and ERRAT servers were employed for residue-by-residue analysis and parameter comparisons against established structural (Venkataraman *et al*., 2023) (Fan *et al*., 2023; Laskowski *et al*., 1993). Additionally, the Ramachandran plot was generated to assess the backbone conformation and identify energetically favorable regions for φ and ψ angles. To further ensure structural integrity, ProSA, an interactive web server, was utilized to screen for potential errors within the 3D model (Wiederstein & Sippl, 2007).

Crystalline structure preparation

The Protein Data Bank (PDB) [RCSB Protein Data Bank, rcsb.org] was queried to retrieve the crystal structure of the human peroxisome proliferator-activated receptor gamma (PPARγ) bound to amorfrutin B (PDB ID: 4A4W). Selection criteria prioritized structures with the highest resolution and minimal missing residues. The 4A4W crystal structure of PPARγ was selected for docking studies based on its high resolution of 2.00 Å and its representation of the active conformation bound to a co-crystallized agonist (amorfrutin B). Alternative structures, such as 2PRG and 3DZY, were evaluated but not chosen due to lower resolution or missing critical regions in the binding domain. The retrieved structure was subsequently prepared for docking simulations using Auto Dock tools. This process involved conversion of the macromolecule (PPARγ) and ligand (amorfrutin B) into the PDBQT file format, suitable for Auto Dock Vina (Agarwal & Mehrotra, 2016). During protein preparation, water molecules were carefully evaluated for their role in protein-ligand interactions. While some water molecules were removed to facilitate docking, key structural waters identified in the crystal structure were retained if they were involved in important hydrogen bonding networks. Hydrogen atoms were added considering appropriate protonation states at physiological pH (7.4), and their positions were optimized using AutoDock tools to minimize potential artifacts.

Ligand library preparation

A total of 342 analogues of eucalyptol were drawn and converted to 3D structures in Chem3D Pro to be exported as pdb files. Autodock tools program from the MGL tools suite was used for further ligand preparation. Polar Hydrogens were added to the structure of all the ligands. The non-polar hydrogens were merged. Finally, the Gasteiger charges were computed. Then the prepared ligands were saved as pdbqt files.

Molecular docking

Molecular docking simulations were performed using AutoDock Vina. The docking grid parameters for the receptor were established based on information gleaned from primary literature on similar ligand-receptor complexes (Acharya *et al*., 2019; Ahmed *et al*., 2014; Bhura *et al*., 2019; Nguyen *et al*., 2022). The grid dimensions (18x18x18 Å) and center coordinates (X: -15.038, Y: 17.760, Z: -12.157) were determined based on the known binding site of amorfrutin B in the 4A4W crystal structure. This binding pocket is well-characterized in the literature for PPAR-γ ligands. The grid box was centered on the co-crystallized ligand's geometric center and expanded to encompass all residues within 10Å of the bound ligand, ensuring complete coverage of the established binding pocket while maintaining computational efficiency. An exhaustiveness value of 10 was selected as it represents an optimal balance between search thoroughness and computational efficiency for our system size, as supported by previous PPAR-γ docking studies. This value is particularly suitable for our ligand library size (342 compounds) and the well-defined nature of the PPAR-γ binding pocket. The energy range was set to 4 kcal/mol to ensure identification of multiple relevant binding modes while excluding high-energy poses unlikely to represent physiologically relevant interactions. This parameter allows AutoDock Vina to report binding modes within 4 kcal/mol of the best binding mode, capturing meaningful alternative conformations while filtering out less probable poses. The validity of the grid and the docking protocol were assessed by comparing the predicted binding modes and scoring functions of eucalyptol.

ADMET

In silico predictions of pharmacokinetic (PK) parameters were performed on top 5 scoring molecules utilizing freely available online software packages. Swiss ADME (Daina *et al*., 2017) was employed to estimate the Absorption, Distribution, Metabolism, and Excretion (ADME) profile of the compounds.

Molecular dynamic simulation

All molecular dynamic simulations and analyses were conducted using a personal computer with CPU of AMD Ryzen 9 7950X 16-Core Processor, 256 GB Ram capacity and GPU of Nvidia GeForce RTX 4090 24GB GDDR6X PCI Express 4.0.

To investigate the dynamic behavior and stability of the top five scoring ligand-protein complexes, we employed molecular dynamics (MD) simulations using GROMACS 2021.4 software. The AMBER 99 SB force field was chosen for its reliable representation of intra-complex atomic interactions. The simulations followed previous methodologies which began with an NVT (constant number of particles, volume, and temperature) equilibration step at 300 K for 1 ns. This step mimicked physiological conditions and ensured complex stability before production dynamics (Rebhi *et al*., 2024). Subsequently, a production MD simulation was run for 100 ns, saving the trajectory every 50 ps (picoseconds) for a total of 2000 frames. This extensive sampling facilitated a comprehensive analysis of the complex's dynamic behavior throughout the simulation.

Following the MD simulation, we analyzed various key properties of the ligand-protein complex from the collected trajectory data. Root Mean Square Deviation (RMSD) and Root Mean Square Fluctuation (RMSF) plots were generated to assess the complex's stability and conformational changes. Additionally, the Radius of Gyration (Rg) provided insights into the overall compactness of the complex. Finally, binding free energies were predicted using the MM-GBSA and MM-PBSA methods, offering a quantitative measure of the ligand-protein interaction strength. These combined analyses provided a comprehensive understanding of the complex's behavior and its potential as a drug target.

RESULTS

Analysis of the protein structure using Procheck revealed favorable Ramachandran angles for 93.3% of residues, indicating a well-defined backbone conformation (fig. 1A). Only 6.7% of residues fell within the allowed regions, with none in the generously allowed or disallowed regions. This suggests a high degree of stereochemical quality suitable for further molecular docking and analysis. The overall quality of the complex was further confirmed by a Z-score of -9.03 obtained through PROSA analysis (fig. 1B and 1C). This score reflects the deviation of the complex's overall energy from the expected energy distribution for well-folded proteins, with lower scores indicating higher quality. Finally, ERRAT analysis, which identifies errors in protein structures by comparing observed atom distributions to those expected in random models, yielded a score of 98.824% (fig. 1D). This high score further supports the structural integrity of the complex.

Eucalyptol served as the control molecule, exhibiting an affinity value of -5.7 kcal/mol. It formed a pi-cation interaction with PPAR-γ at residue Arg288 and hydrophobic interactions with Phe226, Leu228, Leu333, Leu330, Met329, Ile326, Ala292, Ile341, Leu340, Val339, Cys285, Ile281, Phe363, Met364, and Leu353. Glycine bonding was observed with Gly284. The top five molecules with higher affinity than eucalyptol was chosen for further investigation (fig. 2). Notably, all five displayed various degrees of similar hydrophobic interactions with the target protein docked to the control molecule (fig. 3). The molecule AA055 displayed the best affinity out of the entire library at -8.4 kcal/mol while forming hydrophobic bonds at ILE 326, LEU 330, ALA 292, MET 364, LEU 333, CYS 285, ILE 341, LEU 340, and VAL 339. While similarly to the control molecule, formed a glycine bond with GLY 284. While also forming a hydrogen bond at SER 342. The second best molecule, AA051, displayed hydrophobic bonds at residues ILE 341, LEU 340, LEU 330, VAL 339, MET 364, and CYS 285. A hydrogen bond was formed at SER 342 and glycine bond at residue GLY 284. The third ranked molecules, WW040, formed hydrophobic bonds at residues MET 364, ILE 341, LEU 340, VAL 339, ILE 281, CYS 285, ILE 326, and LEU 330. Two hydrogen bonds were formed at ILE 281 and SER 342, while a glycine bond was observed at GLY 284. The fourth ranked molecules, 0Z082, formed hydrophobic bonds at residues ALA 292 LEU 228, LEU 333, LEU 330, MET 329, ILE 326, and CYS 285. A hydrogen bond was formed at ARG 288. Lastly, the fifth best ranked molecule, 0Z114, formed hydrophobic bonds at ILE 296, ALA 292, LEU 228, PHE 226, MET 329, and LEU 333. A hydrogen bond was formed at residue LEU 228.

The functional groups present in each ligand play a critical role in determining their binding affinity and interaction specificity with the PPARγ receptor (table 1). Carbonyl groups, present in ligands AA055, AA051, WW040, and OZ114, serve as key hydrogen bond acceptors. These groups form strong hydrogen bonds with polar residues such as SER 342 and LEU 228, contributing to the stability of the ligand-receptor complex. This interaction highlights the importance of polar functional groups in establishing specific contacts that are critical for receptor activation. Additionally, the ether linkage in OZ082 interacts with ARG 288 through hydrogen bonding, where the oxygen atom acts as a hydrogen bond acceptor. This polar interaction enhances the binding specificity of OZ082 and distinguishes it from other ligands lacking such functionality. Aromatic rings, observed in all ligands, are another crucial feature that facilitates both hydrophobic interactions and Pi-cation interactions. In ligands such as AA051, OZ082, OZ114, and the control molecule Eucalyptol, aromatic rings interact with hydrophobic residues like LEU 330, ILE 326, MET 364, and LEU 228. These interactions stabilize the ligand within the receptor's hydrophobic pocket. In the case of Eucalyptol, the aromatic

ring forms a Pi-cation interaction with ARG 288, which adds an electrostatic stabilization component to the binding interaction. Such interactions are highly sensitive to the spatial orientation of the aromatic systems and are often influenced by the ligand's structural rigidity. The presence of aliphatic chains in OZ082 and OZ114 further enhances their hydrophobic interactions with residues such as ALA 292, LEU 228, and MET 329. These non-polar groups complement the hydrophobic environment of the receptor's binding pocket, improving ligand stability and binding efficiency. The combination of polar and non-polar functional groups in these ligands ensures that they establish both specific and non-specific interactions, thereby improving their overall binding affinity.

The stereochemistry of the ligands significantly influences their biological activity and binding efficiency by determining the precise spatial orientation of functional groups. For ligands such as AA055, AA051, and WW040, the presence of a carbonyl group facilitates hydrogen bonding with SER 342. However, subtle stereochemical variations, such as the orientation of methyl groups or the aromatic backbone, can influence how well these ligands align within the receptor's binding pocket. Differences in orientation may alter the strength of hydrophobic interactions with residues like ILE 326 and LEU 330, thereby impacting binding affinity. In the case of OZ082, the ether linkage introduces a specific spatial requirement for interaction with ARG 288. Stereoisomeric variations in the orientation of the ether oxygen can affect its ability to act as a hydrogen bond acceptor, which may alter the ligand's binding efficiency. Similarly, for OZ114, the alignment of its carbonyl group with LEU 228 and the positioning of its aliphatic chains determine the extent of hydrophobic contacts with residues such as ILE 296 and MET 329. Any stereo chemical differences among its isomers could influence these interactions, resulting in varying degrees of receptor activation. For Eucalyptol, the rigid structure of the cyclic ether and its stereochemistry are critical for forming the Pi-cation interaction with ARG 288. This interaction relies on the proper alignment of the aromatic ring within the receptor's binding pocket. Stereoisomeric changes in the cyclic structure could disrupt this alignment, reducing the strength of the Pi-cation interaction and, consequently, the ligand's binding efficiency.

In silico predictions of key absorption, distribution, metabolism, excretion, and toxicity (ADMET) parameters were performed on the top five scoring molecules using Swiss ADME software (table 2). These analyses provided crucial insights into the pharmacokinetic and safety profiles of the potential PPAR-γ agonists. The comprehensive ADME analysis reveals favorable drug-like properties across all compounds. The consistent high GI absorption, coupled with varied BBB permeability, suggests these compounds could provide both local intestinal and systemic effects.

Bioavailability, a critical determinant of a drug's therapeutic efficacy, was assessed using Swiss ADME's bioavailability score. Notably, all five compounds exhibited favorable scores exceeding 0.55, indicative of high probable oral bioavailability. Notably, OZ114 displayed a superior predicted bioavailability of approximately 0.85, surpassing that of the parent compound eucalyptol (0.55), suggesting a significant probability of achieving adequate systemic exposure following oral administration as well as indicating potential for enhanced therapeutic efficacy.

Evaluation of solubility, an essential prerequisite for adequate absorption and distribution, revealed that all compounds were classified as soluble by SwissADME's ESOL prediction model. Furthermore, the predicted gastrointestinal (GI) absorption probability for all five hits was high, augmenting their potential for oral bioavailability.

The ability to penetrate the blood-brain barrier (BBB) is a desirable attribute for therapeutic agents targeting neuroinflammatory conditions associated with ulcerative colitis. Swiss ADME predictions indicated that three compounds, AA055, AA051, and 0Z082, exhibited favorable BBB permeability, suggesting their potential to exert central nervous system (CNS) effects. Conversely, WW040 and 0Z114 were predicted to be non-permeable to the BBB, limiting their utility in treating neurological complications of ulcerative colitis.

Compliance with Lipinski's Rule of Five, a widely accepted filter for drug-likeness and bioavailability, was assessed using Swiss ADME. Remarkably, all five compounds satisfied Lipinski's criteria, with zero violations reported, further reinforcing their potential for favorable pharmacokinetic profiles. The complete compliance with Lipinski's rules across all compounds supports their viability as drug candidates.

To evaluate the synthetic accessibility and feasibility of large-scale production, Swiss ADME's synthetic accessibility scores were calculated. AA051, WW040, and 0Z114 exhibited scores ranging from 3.65 to 4.44, indicating moderate synthetic complexity, while AA055 and 0Z082 scored 4.19 and 5.88, respectively, suggesting greater synthetic challenges.

Complementary to the ADME predictions, potential toxicological liabilities were assessed using pkCSM software. Preliminary analyses did not reveal any significant toxicity concerns, although more comprehensive in vitro and in vivo toxicological evaluations would be necessary to establish the safety profiles of these compounds conclusively.

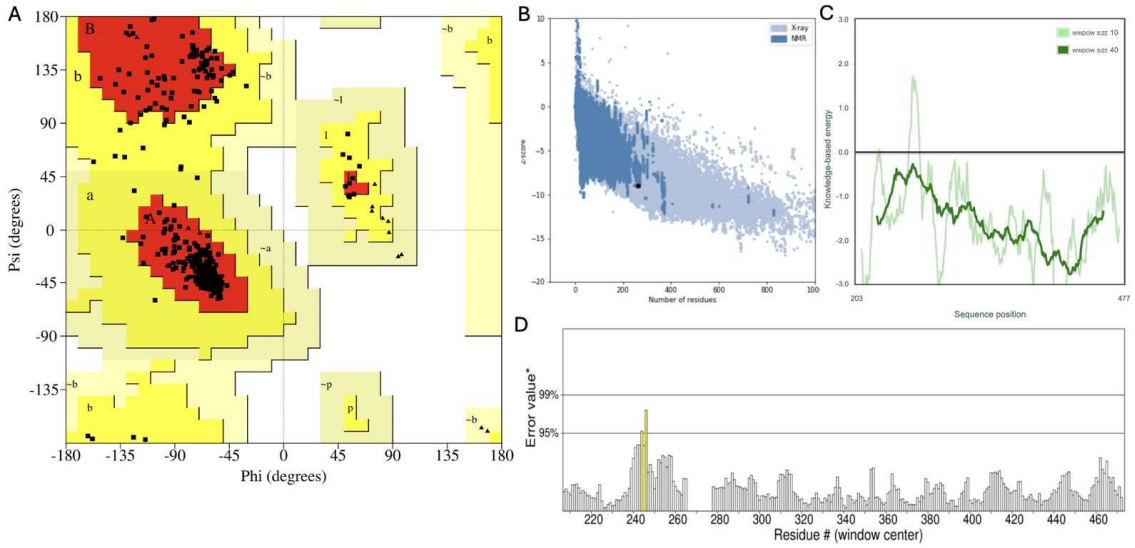

Fig. 1: Structural validation of PPAR-γ. (A) Ramachandran plot showing 93.3% residues in most favored regions (dark blue), 6.7% in allowed regions (light blue), and no residues in disallowed regions, exceeding quality benchmarks for high-resolution structures. (B,C) ProSA analysis revealing Z-score of -9.03, indicating optimal energy distribution compared to experimental structures; energy profile shows no regions of significant instability. (D) ERRAT analysis yielding 98.824% overall quality factor, with no regions showing significant errors in non-bonded atomic interactions. Grey bars indicate mid-range, white bars indicate high-reliability regions.

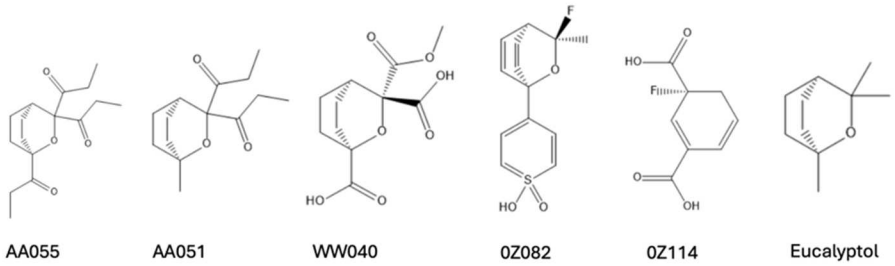

Fig. 2: 2D Structure of top 5 docked compounds and control molecule, Eucalyptol

Table 1: Important interactions of best docked ligands and control

Ligand	Interaction Type	Receptor Residue	Structural Feature of Ligand
AA055	Hydrogen bond	SER 342	Carbonyl group
	Hydrophobic interaction	ILE 326, LEU 330, ALA 292, MET 364, LEU 333, CYS 285, ILE 341, LEU 340 and VAL 339	Rest of the structure
AA051	Hydrogen bond	SER 342	Carbonyl group
	Hydrophobic interaction	ILE 341, LEU 340, LEU 330, VAL 339, MET 364 and CYS 285	Rest of the structure
WW040	Hydrogen bond	SER 342	Carboxyl group
	Hydrophobic interaction	MET 364, ILE 341, LEU 340, VAL 339, ILE 281, CYS 285, ILE 326 and LEU 330	Rest of the structure
OZ082	Hydrogen bond	ARG 288	Ether linkage
	Hydrophobic interaction	ALA 292 LEU 228, LEU 333, LEU 330, MET 329, ILE 326 and CYS 285	Rest of the structure
OZ114	Hydrogen bond	LEU 228	Carboxyl group
	Hydrophobic interaction	ILE 296, ALA 292, LEU 228, PHE 226, MET 329, and LEU 333	Rest of the structure
Eucalyptol	Pi-cation interaction	Arg 288	Ether Linkage
	Hydrophobic interaction	Phe226, Leu228, Leu333, Leu330, Met329, Ile326, Ala292, Ile341, Leu340, Val339, Cys285, Ile281, Phe363, Met364, Leu353	Rest of the structure

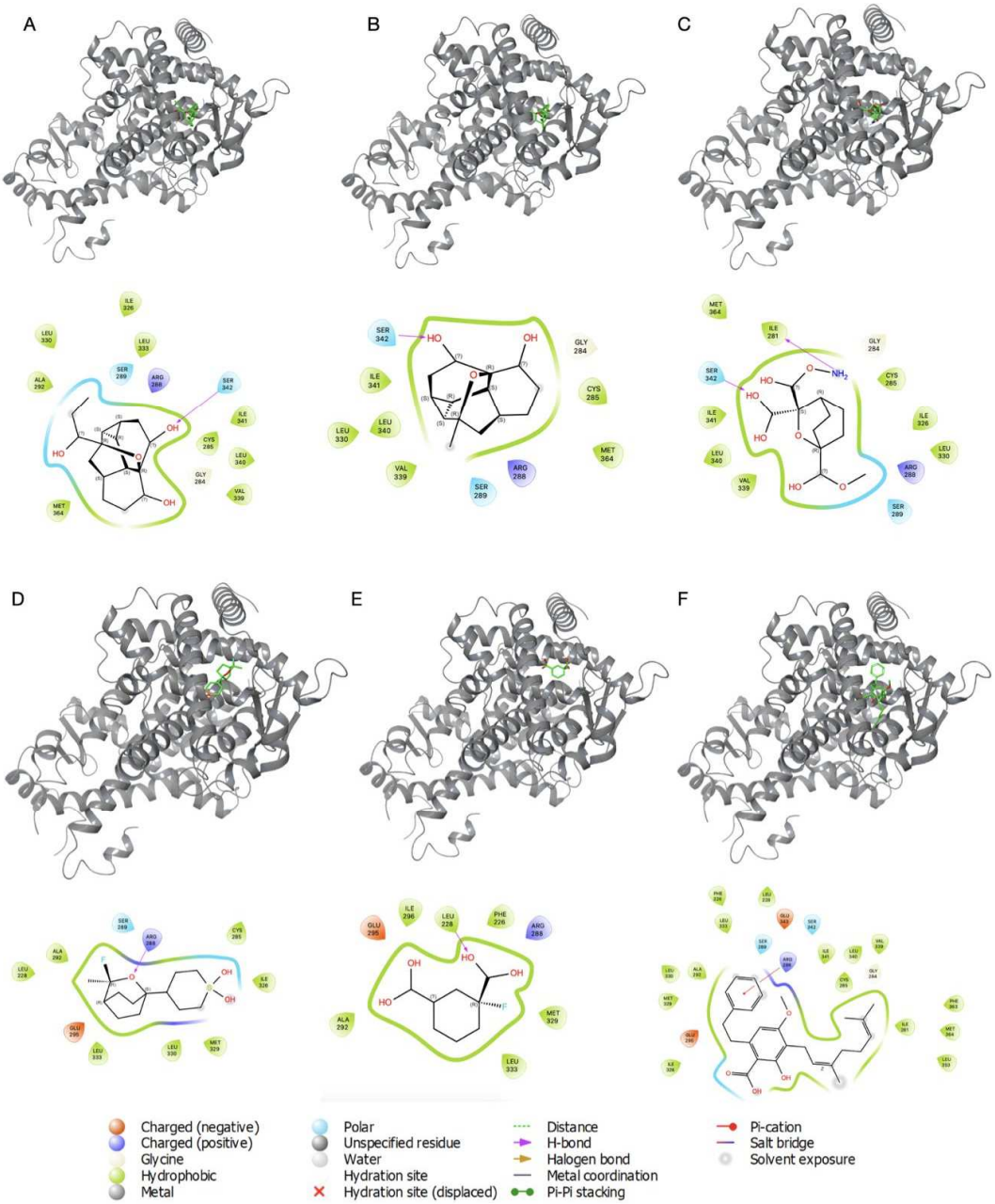

Fig. 3: Visualization of docked compounds and ligand interaction diagram AA055 (A) AA051 (B) WW040 (C) 0Z082 (D) 0Z114 (E) Eucalyptol (F)

Table 2: ADME parameters

	AA055	AA051	WW040	0Z082	0Z114	Eucalyptol
Molecular Weight (g/mol)	280.36	238.32	258.22	268.30	186.14	154.25
TPSA	43.37 Å²	60.44 Å²	110.13 Å²	54.91 Å²	74.60 Å²	9.23 Å²
ESOL Class	Soluble	Soluble	Soluble	Soluble	Soluble	Soluble
GI absorption	High	High	High	High	High	High
BBB permeant	Yes	Yes	No	Yes	No	Yes
log Kp (cm/s)	-6.69	-6.31	-7.66	-7.55	-6.78	-5.3
Lipinski #violations	0	0	0	0	0	0
Bioavailability Score	0.55	0.55	0.56	0.55	0.85	0.55
Synthetic Accessibility	4.19	3.92	4.44	5.88	3.65	3.65

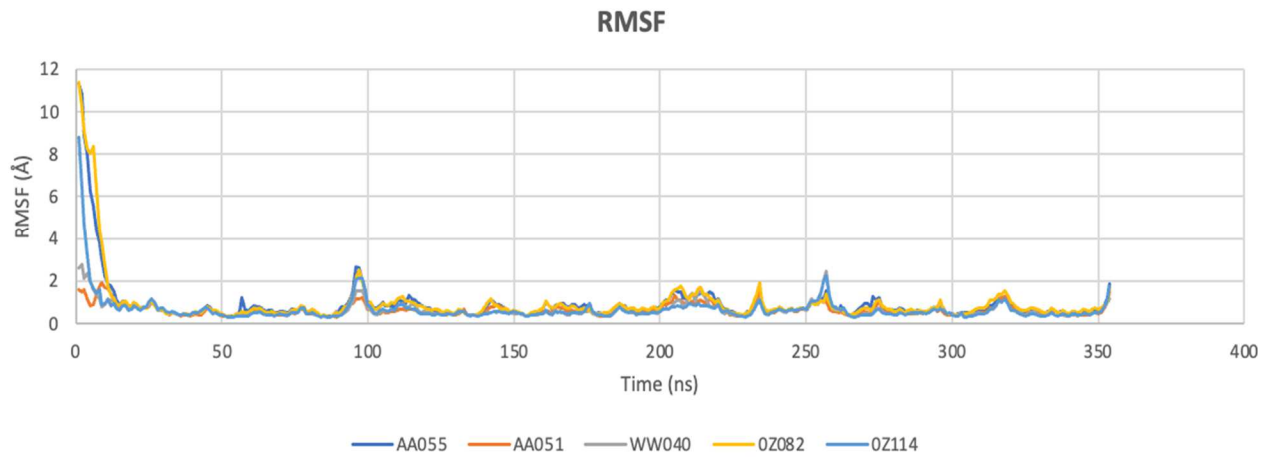

Fig. 4: RMSF

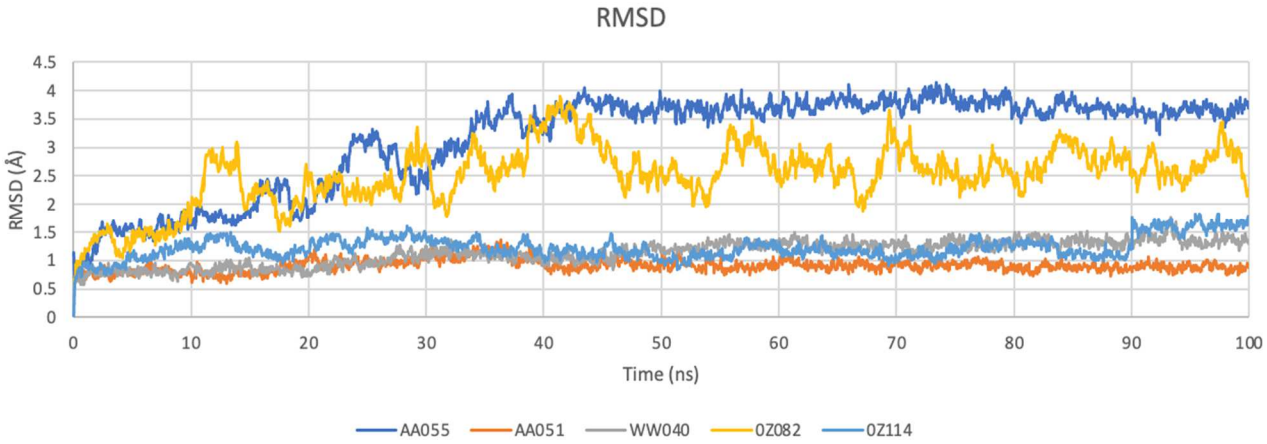

Fig. 5: RMSD

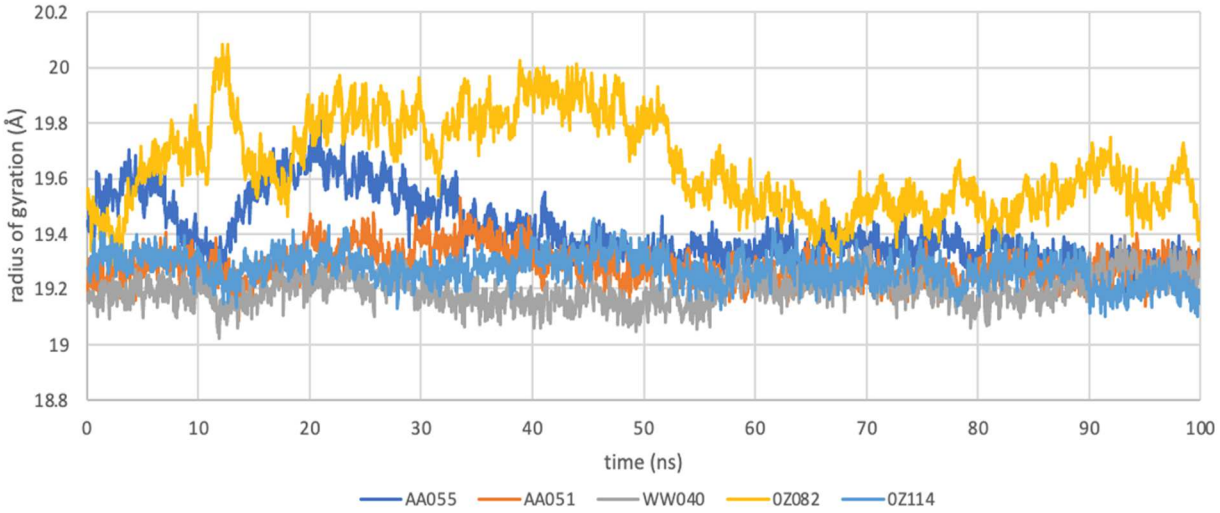

Fig. 6: Radius of gyration

Table 3: MMGBSA and MMPBSA calculations

Protein-Ligand	MMGBSA DELTA TOTAL	MMGBSA Std. Dev.	MMGBSA Std. Err. of Mean	MMPBSA DELTA TOTAL	MMPBSA Std. Dev.	MMPBSA Std. Err. of Mean
AA055	-22.1701	10.6981	3.3830	-13.5451	11.1302	3.5197
AA051	-31.1603	2.8744	0.9090	-16.5293	5.4665	1.7287
WW040	25.8498	3.3964	1.0740	10.7714	5.3819	1.7019
0Z082	6.0276	4.7877	1.5140	14.1335	6.8353	2.1615
0Z114	33.6096	6.9400	2.1946	29.0015	10.2681	3.2471

Molecular dynamics

Our investigation into protein dynamics revealed a significant influence on their function. Root Mean Square Fluctuation (RMSF) analysis provided insight into the protein flexibility, highlighting regions with substantial conformational changes (fig. 4). Interestingly, the overall flexibility across complexes remained comparable. However, residues at positions 1-5 displayed significantly higher RMSF, indicating greater mobility in this region. Additionally, residues 96, 97, and 98 exhibited above-average flexibility.

To evaluate the structural stability and identify potential differences among the five complexes, we performed RMSD analysis. The RMSD profiles over the 100ns simulation showcased distinct patterns (fig. 5). Complexes WW040, AA051, and 0Z114 demonstrated stability throughout the simulation. Conversely, complex 0Z082 exhibited fluctuations from the beginning, achieving relative stability only towards the end (100ns). While complex AA055 achieved stabilization after 40 ns.

The radius of gyration (Rg) analysis provided insights into the overall compactness and shape of the complexes. By comparing the Rg profiles of all complexes, we aimed to identify potential structural variations. While complexes 0Z082 and AA055 displayed initial fluctuations, AA055 reached stability after approximately 43ns. Notably, the remaining three complexes-maintained stability throughout the simulation (fig. 6).

Analysis of molecular dynamics parameters revealed important correlations with known PPAR-γ structural features. The RMSD profiles demonstrated that our most promising compounds, particularly AA051, maintained stability with fluctuations within 2-3Å, consistent with expected thermal fluctuations in nuclear receptors. Complex AA055 showed initial mobility before stabilizing at 40ns, while WW040, AA051, and 0Z114 exhibited immediate stability throughout the simulation.

RMSF analysis highlighted biologically relevant flexibility patterns. The observed higher mobility in residues 1-5 (RMSF peaks of 2.0-4.0Å) and residues 96-98 aligns with known flexible regions in PPAR-γ structure. The magnitude of these fluctuations provides validation of our simulation protocol and suggests preservation of natural protein dynamics during ligand binding.

Radius of gyration measurements demonstrated maintenance of PPAR-γ's compact globular structure. While complexes 0Z082 and AA055 showed initial fluctuations, AA055 achieved stability after approximately 43ns. The remaining three complexes maintained consistent Rg values within 0.5Å throughout the simulation, indicating preservation of the protein's structural integrity during ligand binding.

Binding free energy calculation

MMGBSA and MMPBSA calculations revealed significant differences in the binding free energies of the complexes (table 3). Notably, the AA051 complex exhibited the most favorable binding free energy profiles, with MMGBSA and MMPBSA values of -31.16 kcal/mol and -16.53 kcal/mol, respectively. These values suggest strong binding interactions between the ligand and the protein in this complex.

The AA055 complex also displayed promising binding energies, with an MMGBSA value of -22.17 kcal/mol. However, a higher standard deviation (10.69 kcal/mol) indicates a larger spread in the data, suggesting some conformational fluctuations during the simulation. Despite this, the standard error of the mean (3.38 kcal/mol) suggests a statistically significant binding interaction.

Conversely, the 0Z114, 0Z082, and WW040 complex displayed considerably less favorable binding free energies, with MMGBSA and MMPBSA positive values. These positive values suggest a weaker interaction between the ligand and the protein in this complex.

DISCUSSION

The present computational study aimed to identify novel PPAR-γ agonists with therapeutic potential for ulcerative colitis, a debilitating form of inflammatory bowel disease. Peroxisome proliferator-activated receptor gamma (PPAR-γ) has garnered significant interest as a therapeutic target due to its regulatory role in inflammatory processes and immune responses implicated in ulcerative colitis pathogenesis.

Eucalyptol, a naturally occurring monoterpene with reported anti-inflammatory and mucolytic properties, served as the initial query molecule. However, its volatile nature and unfavorable pharmacokinetic profile limit its clinical utility, necessitating the design of more stable and bioavailable analogues. Through an extensive in silico screening campaign involving molecular docking of a library of 342 eucalyptol analogues against the PPAR-γ crystal structure, five top-scoring hits (AA055, AA051, WW040, 0Z082, and 0Z114) were identified with higher predicted binding affinities compared to the parent compound.

Structural validation metrics demonstrate exceptional quality when compared to established benchmarks. The 93.3% of residues in favored Ramachandran regions exceeds the typical threshold of 90% for high-quality structures. The ProSA Z-score of -9.03 falls within the optimal range (-12 to -5) for native proteins of similar size, while our ERRAT score of 98.824% surpasses the 95% threshold for high-resolution structures. The binding energy variations observed between AA051 and AA055 (standard deviations of 2.87 and 10.69 kcal/mol respectively) reflect meaningful differences in binding stability rather than computational artifacts, as evidenced by the consistency across multiple analysis methods.

The lead candidate, AA055, exhibited the most favorable docking score of -8.4 kcal/mol, forming multiple hydrophobic interactions with key residues (Ile326, Leu330, Ala292, Met364, Leu333, Cys285, Ile341, Leu340, and Val339) and a hydrogen bond with Ser342 within the PPAR-γ binding pocket. Furthermore, AA055 displayed a promising ADME profile, characterized by high oral bioavailability, solubility, and blood-brain barrier permeability, suggesting favorable pharmacokinetic properties conducive to systemic exposure and central nervous system penetration.

The ADME parameters of our compounds align well with established benchmarks for oral drug candidates. Optimal TPSA ranges for oral drugs typically fall between 20-140 Å², with values under 140 Å² generally associated with good membrane permeability. Our compounds (ranging from 9.23-110.13 Å²) fall within this range. Bioavailability scores above 0.55 are considered favorable, with scores above 0.80 being excellent. Notably, 0Z114's bioavailability score of 0.85 is particularly promising, while other compounds maintain acceptable scores of 0.55-0.56. Log Kp values between -8.0 and -1.0 are typical for skin permeation, with our compounds (-5.3 to -7.66) falling within this optimal range.

Initial pkCSM toxicity predictions indicate favorable safety profiles for our compounds. All compounds showed no predicted hepatotoxicity, no hERG I inhibition, and low predicted LD50 values comparable to similar approved drugs. However, these computational predictions should be validated through experimental toxicology studies during subsequent development phases.

The ADMET profiles of our compounds present both opportunities and challenges for therapeutic development. The high GI absorption across all compounds is particularly advantageous for ulcerative colitis treatment, ensuring good exposure at the site of action. The selective BBB permeability of AA055, AA051, and 0Z082 could allow addressing potential neuro inflammatory components of UC, while WW040 and 0Z114's BBB impermeability might reduce off-target CNS effects. The excellent bioavailability score of 0Z114 (0.85) suggests potential for reliable oral dosing, though its lower binding affinity compared to AA051 presents a development trade-off. Future optimization efforts should focus on maintaining these favorable ADMET properties while enhancing target engagement.

Molecular dynamics (MD) simulations, employed to evaluate the conformational stability and dynamic behavior of the top-scoring ligand-protein complexes, revealed intriguing insights. While AA055 initially exhibited conformational instability, it achieved structural stabilization after approximately 40 nanoseconds (ns) of simulation time. This observation was corroborated by binding free energy calculations, which yielded a less favorable MMGBSA value of -22.17 kcal/mol for AA055 compared to the second-ranked candidate, AA051. However, the relatively low standard error of the mean (3.38 kcal/mol) suggested a statistically significant binding interaction for AA055, warranting further consideration.

The AA051 analogue emerged as the most promising candidate, exhibiting the lowest (most favorable) binding free energies of -31.16 kcal/mol (MMGBSA) and -16.53 kcal/mol (MMPBSA), indicative of strong binding interactions with PPAR-γ. Notably, AA051 displayed conformational stability throughout the MD simulation, further bolstering its potential as a PPAR-γ agonist. Its predicted ADME properties, including high oral bioavailability, solubility, and blood-brain barrier permeability, aligned favorably with the desired pharmacokinetic profile for a therapeutic agent targeting ulcerative colitis.

In contrast, the WW040, 0Z082, and 0Z114 analogues exhibited less favorable binding profiles, with positive MMGBSA and MMPBSA values suggesting weaker interactions with the PPAR-γ receptor. The positive MMGBSA and MMPBSA values for these compounds suggest suboptimal binding profiles, possibly due to weaker hydrogen bonding or insufficient hydrophobic interactions within the receptor's active site. Drug efficacy often relies on achieving a balance between strong receptor interactions and favorable pharmacokinetic properties. The inability of these compounds to consistently stabilize the receptor-ligand complex suggests limited therapeutic

potential without structural optimization. Consequently, these compounds were deemed less attractive targets for further optimization and development as PPAR-γ modulators in the context of ulcerative colitis.

Certain compounds exhibited less favorable binding profiles due to a combination of structural, interactional, and energetic factors that impacted their stability within the receptor binding pocket. Structural features, such as the lack of polar functional groups, excessive bulkiness, or high conformational flexibility, often resulted in suboptimal alignment with key residues in the binding site. For instance, compounds like WW040 and OZ114 showed limited hydrogen bonding capacity and insufficient hydrophobic interactions, which are crucial for stabilizing the ligand-receptor complex. Additionally, molecular dynamics simulations revealed that these compounds induced increased receptor flexibility, as indicated by higher RMSF values around the binding site residues, suggesting a destabilizing effect on the protein-ligand complex. Energetically, positive MMGBSA and MMPBSA values indicated significant penalties associated with desolvation and conformational strain, which outweighed the benefits of favorable interactions. These findings suggest that modifying these compounds to include additional hydrogen bond donors or acceptors, reducing steric hindrance, and constraining conformational flexibility could enhance their binding profiles. Exploring these structural limitations provides a roadmap for future optimization efforts, ultimately improving the efficacy and therapeutic potential of these analogues.

The pharmacokinetic properties of the compounds are strongly influenced by their structural features, such as molecular size, lipophilicity, presence of polar functional groups, and conformational flexibility. Smaller compounds with balanced hydrophilic and hydrophobic regions, like OZ114, tend to exhibit better bioavailability and metabolic stability, as they are more soluble and less prone to enzymatic degradation. The presence of polar functional groups, such as hydroxyl or carbonyl groups, enhances solubility and facilitates interactions with transport proteins, contributing to improved absorption and distribution. Conversely, compounds with excessive hydrophobicity or bulky substituents may suffer from poor solubility and reduced permeability, limiting their bioavailability. Additionally, flexible molecules are more likely to adopt conformations that hinder receptor binding or increase susceptibility to metabolic enzymes, reducing their therapeutic efficacy. By analyzing these structural features, future design efforts can focus on incorporating functional groups that strike a balance between stability, solubility and receptor binding, while minimizing factors that negatively impact pharmacokinetics, such as high lipophilicity or excessive flexibility.

The present study exemplifies the power of computational approaches in accelerating the drug discovery process, facilitating the identification and prioritization of promising lead compounds for experimental validation. By leveraging an array of in silico techniques, including molecular docking, ADME prediction, and molecular dynamics simulations, we have identified AA051 as a compelling candidate for further optimization and development as a potential therapeutic agent targeting PPAR-γ in ulcerative colitis.

It is important to note that while computational methods provide valuable insights and facilitate the rational design of drug candidates, experimental validation remains crucial. The findings from this study serve as a foundation for subsequent biochemical and biological evaluation of the identified lead compounds, including binding affinity assays, cell-based assays to assess anti-inflammatory activity, and *in vivo* studies to evaluate pharmacokinetic and efficacy profiles. Future studies should involve in vitro binding assays using purified PPAR-γ protein to confirm the predicted binding affinities of AA051. Additionally, in vivo pharmacokinetic studies will have to be conducted to assess the compound's bioavailability, metabolic stability, and toxicity. These experiments will bridge the gap between computational findings and practical applications, offering a comprehensive validation framework.

It is also equally as important to acknowledge that computational methods, while powerful, have inherent limitations. Docking algorithms assume rigid receptor-ligand interactions, which may not fully capture the dynamic nature of binding events. Similarly, MMGBSA and MMPBSA calculations do not account for all entropic contributions. Incorporating enhanced sampling techniques or free energy perturbation methods could improve accuracy in future studies.

Furthermore, the structural insights gleaned from the molecular docking and dynamics simulations can guide future structure-based drug design efforts, enabling the rational modification and optimization of the lead compounds to enhance binding affinity, selectivity, and pharmacokinetic properties.

CONCLUSION

This computational investigation has successfully identified AA051 as a promising PPAR-γ agonist with potential therapeutic applications in ulcerative colitis. The integration of computational techniques has streamlined the lead identification process, paving the way for further experimental validation and optimization of this novel chemical scaffold. The findings underscore the pivotal role of in silico approaches in modern drug discovery endeavors, enabling the efficient exploration of chemical space and accelerating the development of innovative therapeutic strategies for complex diseases such as inflammatory bowel disorders.

Author contributions

M.O. conceived and designed the study. O.K.H., M.A.K., M.W.B.W., M.H., M.A., S.H.A., and C.R.W. performed the experiments. M.O. and C.R.W. wrote the manuscript. O.K.H., M.A.K., M.W.B.W., M.H., M.A., S.H.A., C.R.W., and M.Z. validated findings. M.O. and C.R.W. curated data and edited the draft. M.O. and C.R.W. supervised the study and provided resources/software. All authors have read and agreed to the published version of the manuscript.

Conflict of interest

C.R.W. is employed by Shing Huei Group. All authors declare no conflict of interest.

REFERENCES

Acharya R, Chacko S, Bose P, Lapenna A and Pattanayak SP (2019). Structure based multitargeted molecular docking analysis of selected furanocoumarins against breast cancer. *Sci. Rep.,* **9**(1): 15743.

Agarwal S and Mehrotra R (2016). An overview of molecular docking. *JSM Chem.,* **4**(2): 1024-1028.

Ahmed B, Ashfaq UA, Qamar MTU and Ahmad M (2014). Anticancer potential of phytochemicals against breast cancer: Molecular docking and simulation approach. *Bangladesh J. Pharmacol.,* **9**(4): 545-550.

Bertin B, Dubuquoy L, Colombel JF and Desreumaux P (2013). PPAR-gamma in ulcerative colitis: A novel target for intervention. *Curr. Drug Targets,* **14**(12): 1501-1507.

Bhura N, Gupta J and Gupta P (2019). Molecular docking studies of phytochemicals of basil against SIRT2 as an anti-breast cancer. *Plant Arch.,* **19**(2): 2185-2190.

Caioni G, Viscido A, d'Angelo M, Panella G, Castelli V, Merola C, Frieri G, Latella G, Cimini A and Benedetti E (2021). Inflammatory bowel disease: New insights into the interplay between environmental factors and PPARγ. *Int. J. Mol. Sci.,* **22**(3): 985.

Daina A, Michielin O and Zoete V (2017). SwissADME: A free web tool to evaluate pharmacokinetics, drug-likeness and medicinal chemistry friendliness of small molecules. *Sci. Rep.,* **7**(1): 42717.

Decara J, Rivera P, López-Gambero AJ, Serrano A, Pavón FJ, Baixeras E, Rodríguez de Fonseca F and Suárez J (2020). Peroxisome proliferator-activated receptors: Experimental targeting for the treatment of inflammatory bowel diseases. *Front. Pharmacol.,* **11**: 730.

Fan C, Basharat Z, Mah K and Wei CR (2024). Computational approach for drug discovery against *Gardnerella vaginalis* in quest for safer and effective treatments for bacterial vaginosis. *Sci. Rep.,* **14**: 17437.

Fan C, Memon AAQ, Adhikari P, Osama M and Wei CR (2023). Revisiting the SARS-COV-2 main protease: A 2023 in Silico Odyssey in search of potential inhibitors. *J. Popul. Ther. Clin. Pharmacol.,* **30**(18): 1032-1049.

Fang J, Wang H, Xue Z, Cheng Y and Zhang X (2021). PPARγ: The central mucus barrier coordinator in ulcerative colitis. *Inflamm. Bowel Dis.,* **27**(5): 732-741.

Ferretti F, Cannatelli R, Monico MC, Maconi G and Ardizzone S (2022). An update on current pharmacotherapeutic options for the treatment of ulcerative colitis. *J. Clin. Med.,* **11**(9): 2302.

Gajendran M, Loganathan P, Jimenez G, Catinella AP, Ng N, Umapathy C, Ziade N and Hashash JG (2019). A comprehensive review and update on ulcerative colitis. *Dis. Mon.,* **65**(12): 100851.

Hoch CC, Petry J, Griesbaum L, Weiser T, Werner K, Ploch M, Verschoor A, Multhoff G, Dezfouli AB and Wollenberg B (2023). 1, 8-cineole (eucalyptol): A versatile phytochemical with therapeutic applications across multiple diseases. *Biomed. Pharmacother.,* **167**: 115467.

Izham MNM, Hussin Y, Rahim NFC, Aziz MNM, Yeap SK, Rahman HS, Masarudin MJ, Mohamad NE, Abdullah R and Alitheen NB (2021). Physicochemical characterization, cytotoxic effect and toxicity evaluation of nanostructured lipid carrier loaded with eucalyptol. *BMC Complement. Med. Ther.,* **21**: 1-17.

Kim IS, Silwal P and Jo EK (2023). Peroxisome proliferator-activated receptor-targeted therapies: Challenges upon infectious diseases. *Cells,* **12**(4): 650.

Laskowski RA, Moss DS and Thornton JM (1993). Main-chain bond lengths and bond angles in protein structures. *J. Mol. Biol.,* **231**(4): 1049-1067.

Nguyen TK, Nguyen TNL, Nguyen K, Nguyen HVT, Tran LTT, Ngo TXT, Pham PTV and Tran MH (2022). Machine learning-based screening of MCF-7 human breast cancer cells and molecular docking analysis of essential oils from *Ocimum basilicum* against breast cancer. *J. Mol. Struct.,* **1268**: 133627.

Rebhi S, BZ, Wei CR, Lebbal S, Najjaa H, Sadfi-Zouaoui N and Messaoudi A (2024). Core proteome mediated subtractive approach for the identification of potential therapeutic drug target against the honeybee pathogen *Paenibacillus larvae*. *Peer J.,* **12**: e17292.

Venkataraman B, Almarzooqi S, Raj V, Bhongade BA, Patil RB, Subramanian VS, Attoub S, Rizvi TA, Adrian TE and Subramanya SB (2023). Molecular docking identifies 1,8-Cineole (eucalyptol) as a novel PPARγ agonist that alleviates colon inflammation. *Int. J. Mol. Sci.,* **24**(7): 6160.

Wiederstein M and Sippl MJ (2007). ProSA-web: interactive web service for the recognition of errors in three-dimensional structures of proteins. *Nucleic Acids Res.,* **35**(suppl_2): W407-W410.

Wei CR, Osama M and Tahir S (2025). A narrative overview of retinoid X receptor inhibitors in chronic disease management. *Curr. Drug Res. Rev.,* **17**(3): 333-342.